Proc. Natl. Acad. Sci. USA
Vol. 85, pp. 7892–7896, November 1988
Biochemistry

Messenger RNA structure and gene regulation at the translational level in *Escherichia coli*: The case of threonine:tRNA^{Thr} ligase

(structure probing/tRNA-related structure/derepressed mutants)

HERVE MOINE*, PASCALE ROMBY*, MATHIAS SPRINGER†, MARIANNE GRUNBERG-MANAGO†, JEAN PIERRE EBEL*, CHANTAL EHRESMANN*, AND BERNARD EHRESMANN*‡

*Laboratoire de Biochimie, Institut de Biologie Moléculaire et Cellulaire du Centre National de la Recherche Scientifique, 15 rue René Descartes, 67084 Strasbourg, France; and †Institut de Biologie Physico-Chimique, 13 rue Pierre et Marie Curie, 75005 Paris, France

Contributed by Marianne Grunberg-Manago, July 6, 1988

ABSTRACT **Previous work showed that the expression of the *Escherichia coli* threonine:tRNA^{Thr} ligase (EC 6.1.1.3)-encoding gene (*thrS*) is negatively autoregulated at the translational level and that a region called the operator that is located between 10 and 50 base pairs upstream of the translation initiation codon of the *thrS* gene is directly involved in that control. The conformation of an *in vitro* synthesized RNA fragment extending over the *thrS* regulatory region has been investigated using chemical and enzymatic probes. This study shows that the RNA folds into four well-defined secondary-structure domains, one of them displaying structural similarities to the anticodon arm of tRNA^{Thr}. The conformation of three constitutive mutants containing single base changes in the operator region leading to the loss of the regulatory control was also investigated. The replacement of a base in the anticodon-like loop does not induce any conformational change, suggesting that the residue concerned is directly involved in the regulatory process. However, single mutations in or close to the anticodon-like stem result in a partial or complete reorganization of the structure of the operator region. These rearrangements should affect the binding of the ligase to the operator, leading to loss of the regulatory process.**

In addition to the classical transcriptional regulation of gene expression, an increasing number of phage, bacterial, and eukaryotic genes appears to be regulated at the level of translation (1–5). In many cases the control has been characterized as a negative autoregulation involving a repressor protein acting at specific control sites of the target genes or operons. However, little is known about the mechanism by which translation is controlled or about the structure of the mRNA region involved in the regulatory protein recognition. In bacteria, secondary structure information has been provided for some of the ribosomal protein operator regions by computer predictions and by nuclease probing experiments (6–8).

In the present work, we have investigated in detail the conformation of a mRNA fragment obtained by *in vitro* transcription, containing the translational operator of the threonine:tRNA^{Thr} ligase (EC 6.1.1.3). Previous work has clearly shown that the expression of the threonine:tRNA^{Thr} ligase gene (*thrS*) is negatively autoregulated at the translational level (9, 10). By a genetic approach, Springer *et al.* (11) have defined the *thrS* translational operator as a region located between 10 and 50 nucleotides (nt) upstream of the translational initiation codon and more than 100 bases downstream of the transcription initiation site. Our results show that the region located upstream to the initiation codon is organized in four distinct structural domains. One of these domains, which corresponds to the genetically defined operator, shares several primary- and secondary-structure features with the anticodon arm of some tRNA^{Thr} isoaccepting species. Similar studies were conducted on three mutant mRNAs containing single base changes in the operator region leading to a total loss of the regulatory control. This study establishes a direct correlation between structural aspects and control.

MATERIALS AND METHODS

Preparation of RNA Transcripts. A *Pst* I–*Hin*dIII fragment extending from 1194 base pairs (bp) in front to 57 bp after the initiator AUG of *thrS* was cloned from λMBXΔ20-28 and its mutant derivatives λMBXΔ20-28 L6-8, M4-11, and M6-1 (11) between the *Pst* I and *Hin*dIII sites of vector M13mp8. A *Hpa* I–*Bgl* II fragment extending from 175 bp in front to 710 bp after the initiator AUG was excised from the M13mp8 recombinants and inserted between the *Sma* I and *Bam*HI sites of pSP65 (12). After cesium chloride purification, the plasmid DNAs were linearized with *Hin*dIII (located 57 bp downstream of the initiator AUG) and transcribed using SP6 RNA polymerase as indicated by the supplier (Promega Biotec, Madison, WI).

The RNAs transcribed *in vitro* from the pSP65 derivatives carrying the *thrS* regulatory regions add about 35 nt to the 5′ end of the *in vivo thrS* transcript. Of these nucleotides, 25 correspond to the distance between the SP6 transcription initiation site and the pSP65–*thrS* boundary (a *Sma* I/*Hpa* I hybrid site), and ≈10 nt correspond to the distance between the *Sma* I/*Hpa* I hybrid site and the *thrS in vivo* transcription initiation site that is located ≈162 nt in front of the translation initiation codon of the gene (11). This synthesized RNA should contain the information for the translational control because the translation of another hybrid mRNA synthesized *in vivo* using the *trp* promoter fused at the same *Hpa* I site to the *thrS* regulatory region was shown to be repressed *in vivo* when the ligase concentration is increased (M.S. and M.G.G., unpublished results).

Probing the RNA Structure. Before the probing experiments, the RNA fragments were renaturated by a 5-min incubation at 50°C in the appropriate buffer, cooled down at 20°C for 30 min, and then placed on ice. A standard assay used 0.5 μg of RNA and 1 μg of tRNA^{Phe} as carrier.

Enzymatic digestion. Digestion with RNase T1 (10^{-3} units), RNase U2 (1 unit), nuclease S1 (25–50 units), and RNase V1 (0.05 units) was at 20°C in 50 mM Tris·HCl, pH 7.5/10 mM $MgCl_2$ (in the presence of 1 mM $ZnCl_2$ for nuclease S1) for 5 and 10 min.

The publication costs of this article were defrayed in part by page charge payment. This article must therefore be hereby marked "*advertisement*" in accordance with 18 U.S.C. §1734 solely to indicate this fact.

Abbreviations: nt, nucleotide(s); CMCT, 1-cyclohexyl-3-(2-morpholinoethyl) carbodiimide metho-*p*-toluene sulfonate; Me_2SO_4, dimethyl sulfate.

‡To whom reprint requests should be sent.

Chemical modification. Modification with dimethyl sulfate (Me_2SO_4): native conditions, 0.25–0.5 μl of Me_2SO_4 in 100 μl of 50 mM sodium cacodylate, pH 7.5/10 mM $MgCl_2$ for 5 and 10 min at 20°C; semi-denaturing conditions, the same conditions but in 100 μl of 50 mM sodium cacodylate, pH 7.5/1 mM EDTA. Modification with diethyl pyrocarbonate: same buffer conditions as for Me_2SO_4 but with 20 μl of diethyl pyrocarbonate for a 15- to 30-min incubation at 20°C. Modification with 1-cyclohexyl-3-(2-morpholinoethyl) carbodiimide metho-*p*-toluene sulfonate (CMCT): 50 μl of CMCT (42 mg/ml) in 200 μl of 50 mM sodium borate, pH 8.0/10 mM $MgCl_2$ for 5 to 30 min at 20°C (native conditions) or 50 mM sodium borate, pH 8.0/1 mM EDTA for 5 to 10 min (semi-denaturing conditions). Reactions were stopped as in ref. 13.

Detection of the modified positions. Modified bases or cuts in the phosphodiester chain were identified by primer extension. The primer was a 5′-end-labeled oligodeoxynucleotide complementary to nucleotides 13–26. Synthesis of the primer, labeling, reverse transcription, and analysis of the generated cDNA fragments were as described (13, 14). Elongation controls were run in parallel in order to detect nicks in the template or pauses of reverse transcription.

RESULTS

Structure probing of the wild-type mRNA and of three constitutive mutant RNAs was performed over 152 nt (between −142 and +10 when +1 is the adenine of the translational initiation codon). All nucleotides were tested at one of their Watson–Crick positions with Me_2SO_4 [adenine (N-1) and cytosine (N-3)] and CMCT [guanine (N-1) and uracil (N-3)]. Position N-7 of adenines involved in stacking or in tertiary interactions was tested with diethyl pyrocarbonate. To estimate the degree of stability of helices, probing was achieved in the presence (native conditions) and in the absence (semi-denaturing conditions) of magnesium. The conformation of the RNAs was also probed with nucleases specific for single-stranded regions (T1, U2, and S1) and for double-stranded or stacked regions (RNase V1). Advantages and limitations of the probing approach have been discussed elsewhere (15). A typical autoradiograph is shown in Fig. 1, and results are summarized on the secondary-structure model of the investigated region, derived from computer predictions and improved with the present probing results (Figs. 2 and 3). For convenience, the RNA has been divided into domains, which will be discussed separately.

Wild-Type mRNA (Fig. 2 *a* and *b*). Helix II [(−49)–(−44)]·[(−18)–(−13)] and helix III [(−42)–(−36)]·[(−28)–(−22)] both require the presence of magnesium to be stabilized. Their low stability is related to a high content in A·U and G·U pairs. The stability of these two helices at 25°C, estimated according to Tinoco *et al.* (16), is only −4.6 and −6.6 kcal/mol (1 cal = 4.184 J), respectively, without taking into account the flanking structures, which should introduce a positive term to the free energy. Helix III is mainly cleaved by RNase V1 on the 5′-strand, and only one cut is observed in helix II on the 3′-strand. Note that the RNase V1 accessibility may provide useful information on the spatial arrangement of the different domains of the RNA. In particular, the absence of cleavage would reflect a steric hindrance effect. Region B (−43) and [(−21)–(−19)] is an interior four-base loop. The high reactivity of U^{-43} at N-3 suggests that this residue is quite exposed to solvent. On the opposite strand, the three nucleotides are reactive at Watson–Crick positions. However, the marginal reactivity of A^{-20} at N-7 together with the increased reactivity of C^{-21} at N-3 under semidenaturing conditions, suggest the existence of an intrinsic conformation in this loop. Loop A [(−35)–(−29)] is a well-defined external seven-base loop. All nucleotides are strongly reactive at their Watson–Crick positions, indicating that they are fully exposed. Strong cleavages are observed

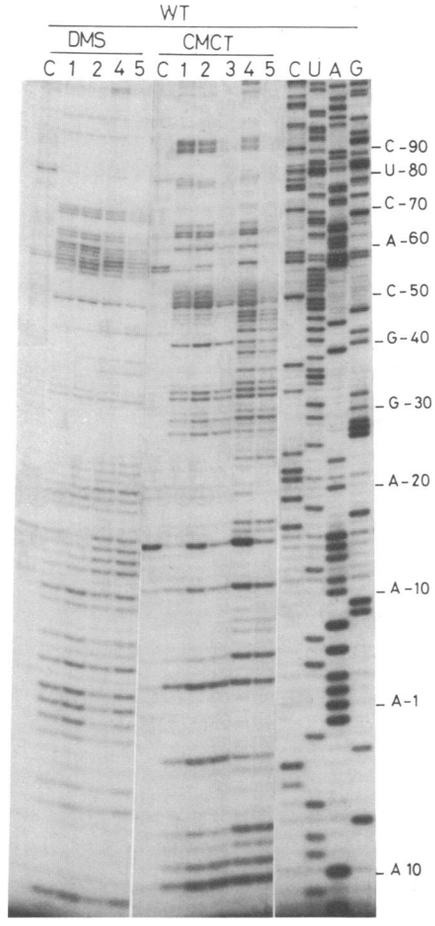

FIG. 1. Gel electrophoresis fractionation of products resulting from Me_2SO_4 (DMS) and CMCT modifications for the wild-type mRNA. Native conditions lanes: C, incubation control; 1, Me_2SO_4 for 2 min and CMCT for 5 min; 2, Me_2SO_4 for 10 min and CMCT for 15 min; 3, CMCT for 30 min. Semi-denaturing conditions lanes: 4, Me_2SO_4 for 2 min and CMCT for 5 min; 5, Me_2SO_4 for 5 min and CMCT for 10 min. Lanes, A, C, G, and U at right correspond to the sequencing products generated in the presence of ddTTP, ddGTP, ddCTP, and ddATP, respectively. At far right wild-type mRNA positions are indicated.

with single-strand-specific nucleases. Comparison with the structure of the different isoacceptors of $tRNA^{Thr}$ shows striking sequence and secondary structure similarities to the anticodon stem and loop (see Fig. 2*a*). In helix IV [(−117)–(−100)]·(−91)–(−74)] most nucleotides are unreactive under native or semi-denaturing conditions, indicating a high stability of the helix, resulting from its high content in G·C pairs. Indeed, the free energy of this helix is estimated at −31 kcal/mol and at −26 kcal/mol with the eight-base exterior loop. The reactivity of U^{-81} at N-3 suggests that this residue is bulging out. The lack of reactivity of U^{-85} at N-3 and the reactivity of A^{-106} and A^{-107} at both N-1 and N-7 suggest an equimolecular mixture of two forms—one displaying a U^{-85}·A^{-106} bp and the other one a U^{-85}·A^{-107} pair. RNase V1 predominantly cleaves the 5′-strand of the helix near the apex, indicating a good accessibility of this area. In the bottom of the helix, a single cut appears at −88. Loop D [(−99)–(−92)] is a well-defined eight-base loop closed by two G·C pairs. All nucleotides are highly reactive to the chemical probes, with the exception of G^{-92} and A^{-99} at N-1 and N-7, respectively. A noncanonical base pair, involving adenine (N-7, N-6) and guanine (N-1, O-6), can be postulated. Such a pairing has been proposed in chloroplastic 5S rRNA (17) and in the *E. coli* 16S rRNA binding site of ribosomal protein

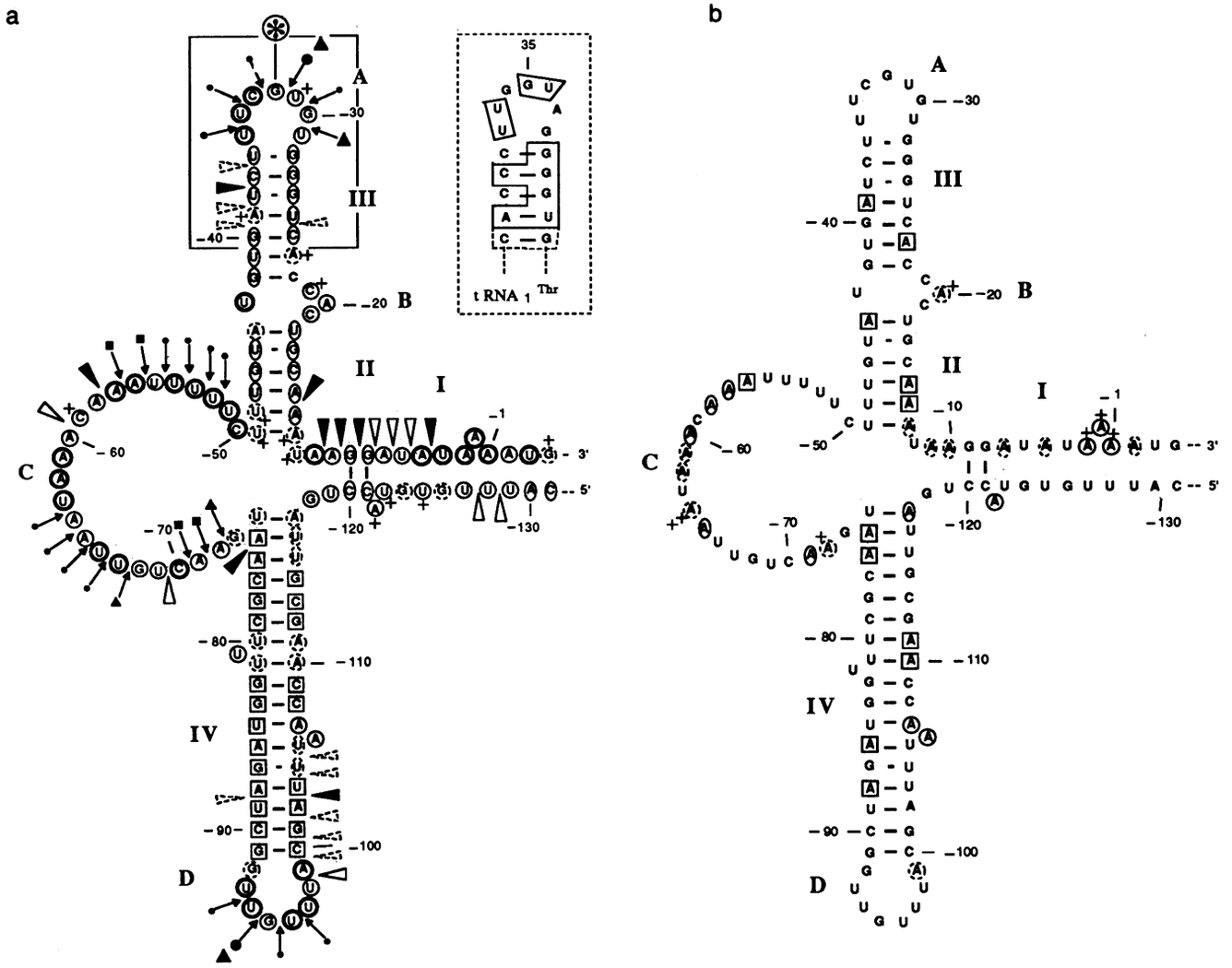

FIG. 2. Reactivity of nt −131 to +3 in the wild-type mRNA and in mutant L6-8. (*a*) Reactivity of Watson–Crick positions and accessibility to enzymatic probes. (*b*) Reactivity of position N-7 of adenines. RNase cuts are indicated by arrows. ▲, RNase T1; ■, RNase U2; ●, nuclease S1; and ▮, RNase V1. The size or intensity of a symbol reflects the rate of nuclease digestion. Reactivity towards Me_2SO_4, CMCT, and diethyl pyrocarbonate: reactive under native conditions (○, strong, moderate, and marginal reactivities are denoted by bold, thin, and dotted symbols, respectively); unreactive under native conditions and reactive under semi-denaturing conditions (◯, low reactivity is denoted by dotted symbol); unreactive under both native and semi-denaturing conditions (□). +, increased reactivity after removal of magnesium. The loops are denoted by A–D and helices by I–IV. The anticodon-like arm in the mRNA is boxed. The inset describes the anticodon region of $tRNA_1^{Thr}$, in which the sequence similarities with the mRNA are framed. In mutant L6-8, G^{32} (denoted by an asterisk) is replaced by adenine. This adenine shows a moderate reactivity at N-1 and a marginal reactivity at N-7 (with an enhanced reactivity under semi-denaturing conditions).

S15 (18). This loop exhibits the major sites of cleavage with nuclease S1 and RNase T1 confirming that all bases are exposed. The presence of RNase V1 cuts that extend the set of cuts observed on the 5′-strand of helix IV may indicate that this side of the loop is stacked on the 5′-strand.

Domain I [(−12)–(+3)],[(−118)–(−131)] that contains the initiation codon (A^1UG) and the Shine–Dalgarno sequence ($U^{-12}AAGGA^{-7}$), and region C [(−73)–(−50)], the hinge region between helices II and IV, present puzzling problems. The two strands in domain I exhibit a complex pattern of reactivity. Different degrees of reactivity at Watson–Crick positions are found under native conditions, from highly reactive ($A^{-5}UAAA^{-1}$) to unreactive (C^{-131}, A^{-130}, C^{-121}, C^{-120}, G^{-9}, G^{-8}, and U^{-6}). In the absence of magnesium, all unreactive bases become reactive, and several others show an increased reactivity (A^{-121}, U^{-122}, U^{-124}, and G^3). A general increased reactivity of adenines is also observed at N-7 in the absence of magnesium (Fig. 2*b*). Strikingly, strong RNase V1 cuts are observed over the Shine–Dalgarno sequence, indicating that this region is highly exposed and revealing an ordered conformation. Indeed, a potential base-pairing is observed between $A^{-10}GGAUAUAAAAUG^2$ and $C^{-131}AUUUGUGUACCU^{-119}$ (with one of the adenines in position −3 to −1 and A^{-122} bulging out). The simultaneous occurrence of RNase V1 cuts and chemical reactivity at Watson–Crick positions most likely indicates that the helix is near its melting point. Therefore, both single-stranded and double-stranded helical forms can be trapped by the probes. Note that another pairing possibility exists between $A^{-10}GGAU^{-6}$ and $A^{-56}UUUU^{-52}$ in loop C. Such a helix has an extremely low stability (−1.8 kcal/mol). Our results do not predict a unique and unambiguous conformation and more likely reflect dynamic properties. Loop C exhibits an overall high reactivity at Watson–Crick positions (with an increased reactivity of C^{-59} under semi-denaturing conditions) and is readily split by single strand-specific nucleases. By contrast, adenines are unreactive at N-7, with two exceptions (A^{-64} and A^{-72}) that become more reactive in the absence of magnesium (with a tremendous increase in the case of A^{-64}), reflecting the existence of stacking or nonca-

nonical base pairs. The presence of three RNase V1 cuts at positions −69, −59, and −57 also confirms this interpretation. The high content of adenine and uracil residues in this region offers several possibilities for base pairing. However, the stability of such interactions is probably very low. It is not very clear whether this region adopts an intrinsic ordered structure or is involved in tertiary long-range interactions with some other part of the RNA transcript. No obvious possibilities can be proposed and as already postulated for region I, a dynamic equilibrium of different conformations cannot be excluded.

Mutant L6-8: $G^{-32} \rightarrow A$ (Fig. 2). The mutation is located in the anticodon-like triplet. Structure mapping at Watson–Crick positions and at N-7 of adenines shows that this mutation does not induce any difference in the reactivity pattern. Nor does the accessibility to nucleases appear either to be modified, with the unique exception of the loss of a T1 RNase cut within the anticodon-like loop, resulting from the replacement of a guanine by an adenine. These results indicate that the conformation of this mutant remains unchanged, compared to the wild-type mRNA.

Mutant M4-11: $C^{-16} \rightarrow U$ (Fig. 3*a*). This mutation destroys the corresponding G·C base pair in the lower part of helix II, resulting in a decreased free energy of the helix (−2.4 instead of −4.6 kcal/mol) when the G·C pair is replaced by a G·U pair. As a consequence of this mutation, the reactivity is essentially altered in helix II. Nucleotides become more reactive at Watson–Crick positions as the result of the destabilization of this helix. The reactivity of A^{-44} is also significantly enhanced at N-7. Nevertheless, the reactivity of adenines −15 to −13 at N-7 is only slightly increased under native conditions and is increased under semi-denaturing conditions. This is accompanied by a decreased RNase V1 cleavage at A^{-15}. Unexpectedly, new cuts are induced around A^{-20} and U^{-48}. This observation is rather difficult to rationalize and might suggest a local reorganization. However, one cannot totally exclude the occurrence of secondary cuts. Besides, the reactivity of the other parts of the transcript is essentially unchanged, indicating that the structure is maintained.

Mutant M6-1: $G^{-40} \rightarrow A$ (Fig. 3*b*). The single change of a guanine involved in a G·C base pair in helix III reduces the stability of the helix from −6.6 to −0.2 kcal/mol. Indeed, this mutation results in an extensive structural rearrangement of region −73 to −13, whereas the region containing helix IV and loop D remains unaltered. In particular, most nucleotides of the anticodon-like loop become unreactive at Watson–Crick positions and are cleaved by RNase V1. Also, a number of nucleotides in region C, which were mostly reactive at Watson–Crick positions in the wild-type RNA, become unreactive in the mutant. The Shine–Dalgarno region is still fully accessible to RNase V1, whereas the reactivity of $A^{-11}AGGAU^{-5}$ is reduced. Although no data are available in region −130 to −115, the postulated helix in region I appears to be stabilized in this mutant, especially the left-hand part. From our results, we propose a secondary structure model of the operator in this mutant, which considerably differs from the wild-type model. In this model, helices II and III and loops A, B, and C are replaced by two new helical structures. The first is a long hairpin with an exterior six-base loop, interrupted by an interior five-base loop. The second, located at the 3′-side of the Shine–Dalgarno sequence, is a five-base pair-helix (possibly containing a noncanonical A·G base pair). The most striking aspect is the complete rearrangement of the nucleotides forming the anticodon-like arm in the wild-type operator (boxed in Fig. 3*b*). Note that G^{-32}, which was found essential in the feedback control is base paired with U^{-74} in this mutant.

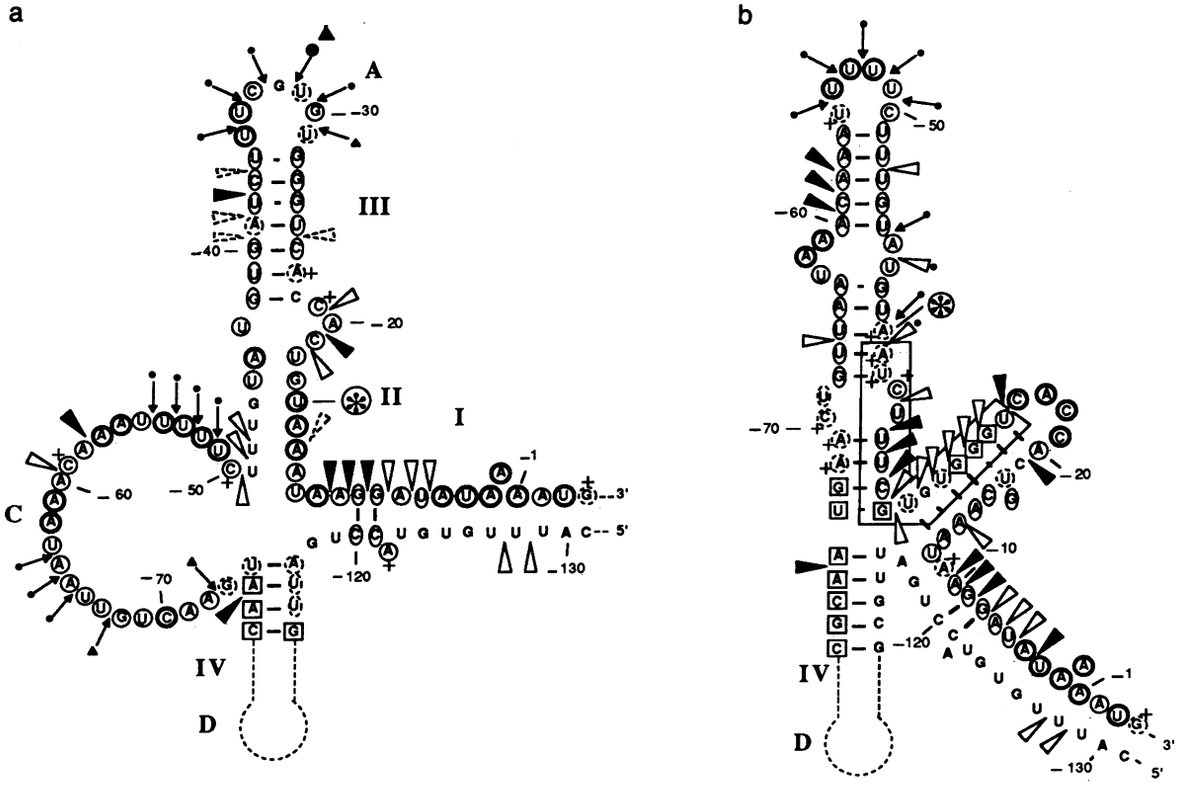

FIG. 3. Reactivity of nucleotides −131 to +3 in mutants M4-11 (*a*) and M6-1 (*b*). Reactivity of Watson–Crick positions and accessibility to enzymatic probes; same symbols as for Fig. 2. The point mutations are located by an asterisk. In mutant M6-1 nucleotides corresponding to the anticodon-like arm in the wild-type mRNA are boxed. Helix IV and loop D in the three mutants are represented by a dotted line, as their reactivity remains unchanged.

DISCUSSION

The present study shows that the mRNA region located upstream of the *thrS* initiation codon folds into four distinct structural domains. First, the Shine–Dalgarno sequence and the initiation codon possibly interact with a complementary sequence located about 30 to 40 nt from the transcription initiation site. The resulting helix is highly unstable and should display dynamic properties. The second domain is defined as a long and stable stem-loop structure, and the third domain is a large bulged loop. The structure of this loop is not well characterized but displays a certain degree of organization. The last domain, which corresponds to the genetically defined operator, contains two weak helices interrupted by an interior loop. The upper helix shares structure similarities with the $tRNA^{Thr}$ isoacceptors. (*i*) It contains a seven-base anticodon-like loop with four nucleotides identical to those of the $tRNA_1^{Thr}$ isoacceptor (Fig. 2*a*). Among the four, two correspond to the nucleotides shared by the anticodon sequence of all known isoacceptors. (*ii*) It contains an anticodon-like helix with several base pairs identical to those of the different $tRNA^{Thr}$ isoacceptors. This suggests that threonine:$tRNA^{Thr}$ ligase controls its own synthesis by interacting with the region that shares structural similarities with its natural substrate. Indeed, threonine:$tRNA^{Thr}$ ligase has been shown to interact with the wild-type mRNA transcript and protects the anticodon-like arm, but also other unexpected regions like helix IV and loop D (unpublished results).

Springer *et al.* (11) have isolated mutants leading to complete loss of control of *thrS* expression. The replacement of G^{-32} in the anticodon-like loop by an adenine does not alter the conformation of the RNA in mutant L6-8. This strongly suggests that G^{-32} is essential for the binding of the threonine:$tRNA^{Thr}$ ligase to the anticodon-like arm. This result has to be correlated with footprinting experiments conducted on the $tRNA_3^{Thr}$–threonine:$tRNA^{Thr}$ ligase complex by Théobald *et al.* (19). This work suggested that G^{35} in the anticodon sequence (analogous to G^{-32} in the anticodon-like triplet) is involved in the formation of the complex. Such an involvement is further confirmed by the fact that the change $G^{35} \rightarrow C$ in *thrU* (the gene for $tRNA_4^{Thr}$) strongly decreases aminoacylation of the corresponding isoacceptor (unpublished results). The crucial role of the anticodon-like arm is further supported by mutant M6-1, in which the mutation-induced rearrangement leads to the disappearance of the anticodon-like arm structure. In the particular case of mutant M4-11, the regulatory control is lost, though the anticodon-like arm is unaltered in sequence and secondary structure. It can be postulated that the destabilization of helix II, which extends the anticodon-like helix, should result in a lack of a correct geometry of the anticodon-like arm. In the case of mutants M4-11 and M6-1, the loss of control is most probably not due to the mutation of an essential residue but to a conformational rearrangement. Especially in the case of M6-1, a single base change causes an extensive rearrangement over 60 nt, which was not predicted by the computer. Therefore, it appears that the conformation of wild-type and mutant RNAs should be investigated in parallel to genetic approaches.

A feedback regulatory mechanism can be imagined, in which the ligase would bind to the mRNA at the region-sharing sequence and structure similarities with $tRNA^{Thr}$, located just upstream of the Shine–Dalgarno sequence, thus preventing the ribosomes from translating the *thrS* mRNA. In line with this, modification of a single base in the anticodon-like loop that is essential for protein binding or a conformational change of the anticodon-like region would affect the binding of the ligase to the operator region, leading to loss of the control. A well-known example of interaction between a ligase and a noncognate substrate is provided by the aminoacylation of the 3′-end of several viral RNAs displaying tRNA-like structures (20, 21). Recently, two mitochondrial amino acid–tRNA ligases, the tyrosine–tRNA ligase of *Neurospora crassa* (22) and the leucine–tRNA ligase of *Saccharomyces cerevisiae* (23) were shown to be directly involved in RNA splicing. This specific property of amino acid–tRNA ligases could also be explained by interactions between the ligase and tRNA-like structures in introns. Thus, tRNA-like structures may be involved in a variety of biological functions such as genomic RNA tagging (24) and the control of gene expression at the levels of both RNA maturation and translation.

Although both genetic and biochemical investigations tell us about the sites that are essential for the modulation of the mRNA translation, precise information about the extent of the mRNA that is recognized by the ligase and the ribosome are required. Both genetic and biochemical experiments are currently in progress to define more precisely the extent of the *thrS* translational operator and the nature of the ligase–mRNA interaction.

We are indebted to M. Mougel and R. Giegé for many fruitful discussions and to F. Eyermann for skillful technical assistance. We are grateful to R. Buckingham for critically reading the manuscript. This work was supported by grants from the Centre National de la Recherche Scientifique (LP6201 and UA1139), from the Fondation pour la Recherche Médicale and E. I. duPont de Nemours (to M.G.-M.), and from Ministére de la Recherche de l'Education Nationale (88.C.0562) (to B.E. and M.S.).

1. Lindahl, L. & Zengel, J. M. (1986) *Annu. Rev. Genet.* **20,** 297–326.
2. Thomas, M. S. & Nomura, M. (1987) *Nucleic Acids Res.* **15,** 3085–3096.
3. Stormo, G. D. (1987) in *Translational Regulation of Gene Expression*, ed. Ilan, J. (Plenum, New York), pp. 27–49.
4. Hentze, M. W., Caughman, S. W., Rouault, T. A., Barriocanal, J. G., Dancis, A., Harford, J. B. & Klausner, R. D. (1987) *Science* **238,** 1570–1573.
5. Leibold, E. A. & Munro, H. N. (1988) *Proc. Natl. Acad. Sci. USA* **85,** 2171–2175.
6. Climie, S. C. & Friesen, J. D. (1987) *J. Mol. Biol.* **198,** 371–381.
7. Deckman, I. C. & Draper, D. E. (1987) *J. Mol. Biol.* **196,** 323–332.
8. Kearney, K. R. & Nomura, M. (1987) *Mol. Gen. Genet.* **210,** 60–68.
9. Springer, M., Plumbridge, J. A., Butler, J. S., Graffe, M., Dondon, J., Mayaux, J. F., Fayat, G., Lestienne, P., Blanquet, S. & Grunberg-Manago, M. (1985) *J. Mol. Biol.* **185,** 93–104.
10. Butler, J. S., Springer, M., Dondon, J. & Grunberg-Manago, M. (1986) *J. Bacteriol.* **165,** 198–203.
11. Springer, M., Graffe, M., Butler, J. S. & Grunberg-Manago, M. (1986) *Proc. Natl. Acad. Sci. USA* **83,** 4384–4388.
12. Melton, D. A., Krieg, P. A., Rebagliati, M. R., Maniatis, T., Zinn, K. & Green, M. R. (1984) *Nucleic Acids Res.* **12,** 7035–7056.
13. Mougel, M., Eyermann, F., Westhof, E., Romby, P., Expert-Bezançon, A., Ebel, J. P., Ehresmann, B. & Ehresmann, C. (1987) *J. Mol. Biol.* **198,** 91–107.
14. Baudin, F., Ehresmann, C., Romby, P., Mougel, M., Colin, J., Lempereur, L., Bachellerie, J. P., Ebel, J. P. & Ehresmann, B. (1987) *Biochimie* **69,** 1081–1096.
15. Ehresmann, C., Baudin, F., Mougel, M., Romby, P., Ebel, J. P. & Ehresmann, B. (1988) *Nucleic Acids Res.* **15,** 9109–9128.
16. Tinoco, I., Borer, P. N., Dengler, B., Levine, M. D., Uhlenbeck, O. C., Crothers, D. M. & Gralla, J. (1973) *Nature (London) New Biol.* **246,** 41–42.
17. Romby, P., Westhof, E., Toukifimpa, R., Mache, R., Ebel, J. P., Ehresmann, C. & Ehresmann, B. (1988) *Biochemistry*, in press.
18. Mougel, M., Philippe, C., Ebel, J. P., Ehresmann, B. & Ehresmann, C. (1988) *Nucleic Acids Res.* **7,** 2825–2839.
19. Théobald, A., Springer, M., Grunberg-Manago, M., Ebel, J. P. & Giegé, R. (1988) *Eur. J. Biochem.*, in press.
20. Hall, T. C. (1979) *Int. Rev. Cytol.* **60,** 1–26.
21. Haenni, A. L., Joshi, S. & Chapeville, F. (1972) *Prog. Nucleic Acids Res. Mol. Biol.* **27,** 85–104.
22. Akins, R. A. & Lambowitz, A. M. (1987) *Cell* **50,** 331–345.
23. Herbert, C. J., Labouesse, M., Dujardin, G. & Slonimski, P. P. (1988) *EMBO J.* **7,** 473–483.
24. Weiner, A. M. & Maizels, N. (1987) *Proc. Natl. Acad. Sci. USA* **84,** 7373–7387.